Segregation and interdiffusion effects during the formation of the Mn/Cd(Zn)Te(100) interface

C. Heske, U. Winkler, R. Fink, and E. Umbach
Experimentelle Physik II, Universität Würzburg, Am Hubland, D-97074 Würzburg, Germany

Ch. Jung and P. R. Bressler
BESSY-GmbH, Lentzeallee 100, D-14195 Berlin, Germany
(Received 25 November 1996)

The formation of the Mn/Cd(Zn)Te(100) interface has been investigated with soft x-ray excited photoelectron and Auger electron spectroscopy. Apart from a metal-semiconductor interface with a valence-band maximum 1.05 (± 0.10) eV below the Fermi energy, several interesting effects such as interface compound formation, Te-segregation, surface photovoltage effects due to metal-induced band bending, and the formation of a secondary Te phase have been observed. The results are discussed in the framework of a layer model. A schematic electronic structure of the Mn/Cd(Zn)Te(100) interface is derived for different Mn coverages. [S0163-1829(97)00428-1]

I. INTRODUCTION

CdTe-based II-VI-compound semiconductors have attracted considerable interest due to their present and potential applications for semiconductor devices. The tunability of band gaps and lattice parameters by concentration variation in ternary compounds is a basic prerequisite for a successful device fabrication with techniques such as molecular beam epitaxy (MBE) or atomic layer epitaxy (ALE). Cd(Zn)Te, for example, is commonly used as a lattice matched substrate to HgTe/CdTe superlattices,[1] which is motivated by the use of Hg-containing II-VI compounds for infrared applications.[2] Frequently, CdTe-layers are grown on commercial Cd(Zn)Te substrates, since the Zn ''doping'' (usually in the range of 4 at. %) increases the electrical conductivity of the contacting substrate. This is also very desirable in synchrotron photoemission experiments, since the high photon flux is concentrated on a small area of incidence, thus frequently leading to charging effects in spectra of low-conductivity (i.e., undoped) samples.

Most photoemission studies of CdTe have been performed on the (110) cleavage plane of the zinc-blende lattice. For MBE or ALE purposes, however, the polar, noncleavage (100) surface is of major importance. Single crystal surfaces of this orientation can be prepared in a well-ordered, clean, stoichiometric, and uniformly terminated way by successive sputter/annealing cycles under various annealing conditions (e.g., under Cd-flux, under Te-flux, and also in UHV).[3–6].

Among the ternary II-VI semiconductors, the semimagnetic, Mn-containing compounds play a prominent role in magneto-optical applications.[7–18] $Cd_{1-x}Mn_xTe$, in particular, has attracted considerable interest, but also interfaces of MnTe with CdTe.[19–32]

We have chosen to investigate the Mn/Cd(Zn)Te(100) interface as a simplified starting-point system for semiconductor heterointerface studies involving Cd(Zn)Te and Mn-containing II-VI compounds. Moreover, as has been pointed out by Wall *et al.*,[33] interdiffusion at the interface of Mn/CdTe(110) leads to the formation of a Cd(Mn)Te alloy at the (110) surface. Further evidence for interdiffusion and segregation effects stem from investigations of noble metal-CdTe or (Hg,Cd)Te interfaces.[34–39] Thus, our investigation aims at a clarification of the interdiffusion and segregation processes and the nature of the growing Mn overlayer on a CdTe-related ternary substrate by employing a larger range of photon energies than in previous studies of the Mn/CdTe(110) interface.[33,40]

II. EXPERIMENT

Photoemission experiments were performed at the plane grating monochromator PM5 (HE-PGM3) beamline[41] of the BESSY synchrotron source using the HIRES spectrometer (base pressure 1×10^{-10} mbar) and a separate MBE chamber (4×10^{-10} mbar). Polar (100) surfaces of commercial, nominally undoped Cd(Zn)Te single crystals with a nominal Zn content of 4% were prepared by 1 keV Ar^+ ion sputtering and annealing under Cd flux (10^{-6} mbar) at 300 °C. After several sputter/annealing cycles, a low-energy electron-diffraction and x-ray photoelectron spectroscopy and (XPS) investigation at room temperature revealed a well-ordered, clean, and stoichiometric $c(2\times2)$-reconstructed surface, which has previously been determined to be Cd terminated for both, CdTe(100) and Cd(Zn)Te(100) surfaces.[3,5,6,42,43] Due to the Zn ''doping'' of the crystal, no charge compensation had to be applied during the photoemission experiments.

Mn deposition was performed at room temperature from a Mn lump held in a resistively heated tungsten wire and monitored with a quartz microbalance prior and after each deposition step. The given nominal Mn film thicknesses derived from the quartz microbalance were verified *in situ* by Mg $K\alpha$ XPS, which has also been used to derive spectra of the *MNN* Auger decays of Cd and Te and of the 3*s* photoemission of the Mn overlayer. Throughout the experiments presented in this paper, checks of surface cleanliness were performed but no oxygen or carbon contaminations could be detected.

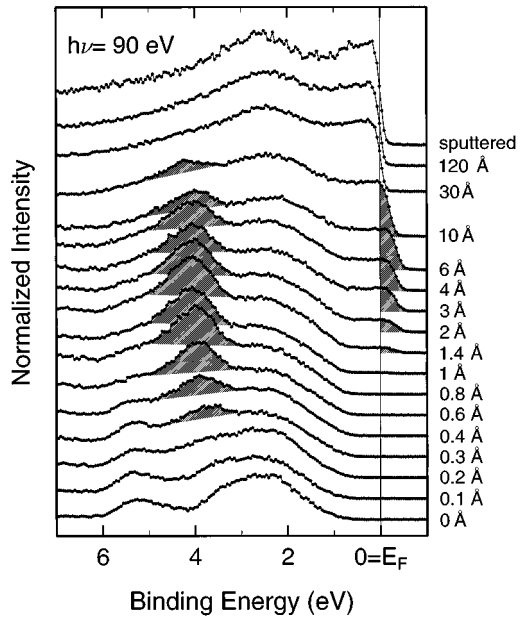

FIG. 1. Photoemission spectra ($h\nu$ = 90 eV) of the valence-band region of Cd(Zn)Te(100) (0 Å Mn), for increasing nominal Mn coverage (0.1–120 Å Mn) and after removal of a few atomic layers by short sputter treatment. Hatched areas denote the formation of a band at $E_B \approx 4$ eV due to a secondary phase and the evolution of the Fermi edge, revealing a surface photovoltage effect for nominal Mn thicknesses between 1 and 10 Å.

III. RESULTS AND INTERPRETATION

A series of successive Mn deposition steps onto a $c(2\times2)$-reconstructed, Cd-terminated Cd(Zn)Te(100) surface is shown for the valence-band region in Fig. 1. With increasing coverage, four different effects can be detected. First, the split-off band of the pristine Cd(Zn)Te between 4 and 6 eV (Refs. 44 and 45) is attenuated. Second, an additional emission feature at approximately 4 eV appears in the intermediate-coverage range (0.3–10 Å) and cannot be detected for large Mn coverages. Third, a Fermi edge can only be resolved for nominal Mn coverages $\geqslant$ 1 Å. Finally, the position of the Fermi edge in the intermediate-coverage range (1–10 Å) is detected well above the Fermi energy of the system, as derived from a gold-foil reference in electrical contact with the sample. This last effect is due to a surface photovoltage, as will be discussed below.

The results of Fig. 1 give evidence for a layer model which is the result of a combination of all data of this paper. This model is briefly introduced in this paragraph in order to facilitate the reading. During the first few deposition steps up to a nominal Mn coverage of 0.8 Å, an interdiffused Cd(Zn,Mn)Te quaternary semiconductor is formed has similarly been reported by Wall *et al.*[33] and confirmed by Happo *et al.*[40] for Mn/CdTe(110). This is derived from the fact that no emission at the Fermi energy can be detected for coverages below 1 Å and from the different attenuation behavior of Cd, Zn, and Te core level emission with increasing Mn coverage (see below in connection with Fig. 6). For the Mn/CdTe(110) interface a metallic Fermi edge is detected only for larger Mn coverage (3 Å)[33,40], which is presumably due to the different surface orientation. For coverages above 1 Å,

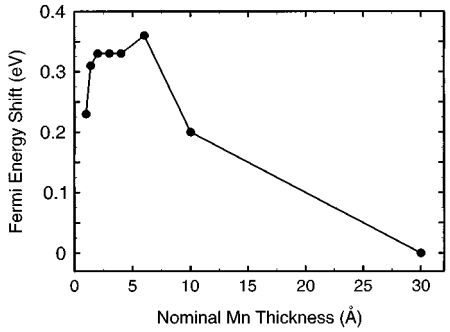

FIG. 2. Surface photovoltage shift of the experimental Fermi edge with respect to the Fermi energy of the instrument, as derived from the photoemission spectra in Fig. 1 ($\pm$0.05 eV). The Fermi energy of the instrument was independently determined from a Au-foil reference in electrical contact with the sample.

a metallic Mn layer is formed, which induces a band bending within the quaternary compound resulting in a surface photovoltage effect[50,51] (Fig. 2) and the formation of a Schottky barrier interface (Figs. 3, 4). In the intermediate coverage range (0.8 Å–10 Å), a second phase (to be named ''Mn-Te phase''), consisting of Mn and Te, is formed on top of the Mn film, as can be deduced from photoemission (Figs. 3, 5) and Auger emission results (Figs. 7, 8) and from the fact that, throughout the Mn deposition, some Te floats on top of the metallic Mn film (Figs. 5, 6). An investigation of the Mn $3s$ and $2p_{3/2}$ core levels is given in Figs. 9 and 10, which reveal two different Mn phases for the first few deposition steps. Finally, in Figs. 11 and 12, the above sketched interface model will be discussed in more detail as a layer scheme including a schematic view on the electronic structure.

Next we discuss the observations derived from Fig. 1. The

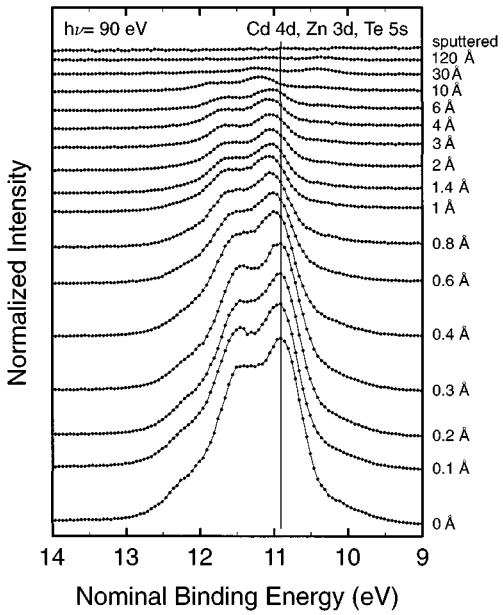

FIG. 3. Photoemission spectra of the Cd $4d$ levels ($h\nu$=90 eV). At higher binding energies (11.8–12.5 eV), the surface-shifted component of the Cd $4d$ signal is visible. Emission from the Te $5s$ signal and the Zn $3d$ levels is superimposed on the low binding energy side of the dominant Cd $4d$ feature.

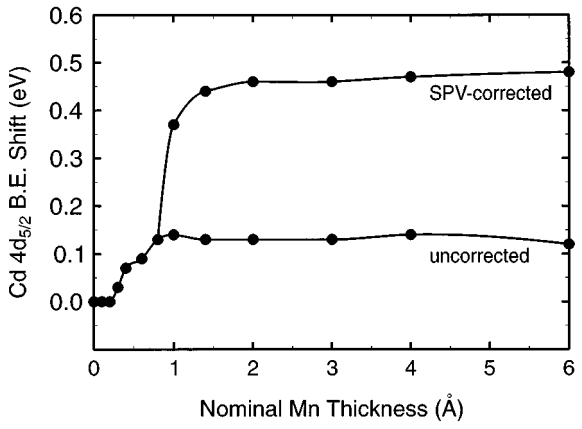

FIG. 4. Binding energy shift of the Cd $4d_{5/2}$ peak with increasing Mn coverage (± 0.05 eV), as derived from Fig. 3 (uncorrected curve). Employing the surface photovoltage correction of Fig. 2, the upper curve is obtained (SPV-corrected). After the initial stage of interface formation a constant downward band bending of approximately 0.5 eV is induced.

additional spectral feature at 4 eV in the intermediate coverage range of Fig. 1 (0.3–10 Å) has frequently been investigated in photoemission studies of semimagnetic II-VI semiconductor compounds. It has been assigned to a Mn $3d$-derived contribution to the density of states by employing a Fano-like Mn $3p$-$3d$ resonant excitation between $h\nu = 47$ and 50 eV, thus enhancing the Mn contribution to the valence-band spectra.[8,9,14–18,22,23,25,28,31,33,40,46,47] However, an unambiguous assignment to a certain chemical state, e.g., in a Mn film, a Mn-Te phase, or a quaternary Cd(Zn,Mn)Te compound is difficult in our case, since an increased Mn-derived emission in this binding energy range is detected for various x values of $Cd_{1-x}Mn_xTe$, including pure MnTe (see, e.g., Refs. 31–33). Moreover, a similar feature at $E_B \approx 4$ eV has been observed for Mn/GaAs(100) and interpreted in terms of an occupancy of the Mn $3d$ majority-spin band of fcc Mn.[48,49] We nevertheless favor the assignment as a quaternary Cd(Zn,Mn)Te compound located at the interface between Cd(Zn)Te bulk and the Mn overlayer, since no emission at 4 eV is detected in the *high*-coverage spectra of Fig. 1. This is compatible with the photoemission information depth, which is then smaller than the Mn overlayer thickness, and with the information that a Mn-Te species is present on the surface (see below).

As already mentioned above, the detection of photoemission intensity above the Fermi energy can be related to a surface photovoltage (SPV) effect, i.e., the generation of charge carriers which are separated by a metal-induced band bending.[50,51] This separation leads to a photon-induced accumulation of positive or negative charge at the interface depending on the direction of band bending. This interpretation of a SPV effect is supported by the fact that for higher Mn coverages ($\geqslant 10$ Å) the Fermi edge is shifted towards higher binding energies. It then coincides with the Fermi energy of the instrument, as is consistent with improved screening by the increasing metallic overlayer. The detection of a Fermi edge at a kinetic energy higher than that of the Fermi energy reference has also been reported by John *et al.* for Ag on *n*-type CdTe(100) in conjuction with a metal-induced downward band bending.[39]

For the determination of the Mn-induced band bending in the underlying semiconductor, the SPV shift of the reference level has, of course, to be taken into account. Figure 2 shows the position of the Fermi edge as derived from the spectra in Fig. 1 with respect to the Fermi energy of the instrument. By employing the SPV correction (i.e., by shifting the spectra towards higher binding energy by the values given in Fig. 2), a simultaneous calibration of the spectra is performed.

The (uncorrected) photoemission spectra of the shallow Cd $4d$ levels are shown in Fig. 3. The spectral feature consists of a superposition of the spin-orbit split Cd $4d_{3/2}$ and $4d_{5/2}$ levels for bulk Cd atoms, the surface-shifted components [which can be seen as a shoulder at higher binding energy between 11.8 and 12.5 eV (Refs. 3, 5, 33, and 52), the Zn $3d$ emission, and the Te $5s$ emission. Zn $3d$ and Te $5s$ peaks show dispersion in $\vec{k}$-resolved studies[29,53] and contribute to the low binding energy side of the Cd $4d$ peaks[45,52,54]. The Cd $4d$ intensity decreases with increasing Mn coverage and can be completely suppressed by thick overlayers. The low-intensity peak at $E_B \approx 10.3$ eV in the 30 and 120 Å spectra is presumably due to Te 5s emission, since there is considerable Te $4d$ emission even for thick Mn layers (see discussion of Figs. 5 and 6). A correlation with segregated Cd as suggested by Wall *et al.* for Mn/CdTe(110) (Ref. 33) can be ruled out, since no Cd $3d$ emission is detected for a nominal Mn thickness of 120 Å.

After removal of the topmost layers by short Ar^+ sputtering no Cd $4d$ emission is detected (topmost spectrum); hence no Cd is dissolved in the Mn layer within the detection limits of photoemission ($\approx 0.1\%$). Moreover, no evidence for the formation of a second, Cd-containing species in the intermediate coverage range is found. However, the peaks are shifted towards higher binding energies for nominal Mn coverages above 0.3 Å, suggesting a downward band bending. Note that the spectra shown are not corrected for the SPV effect, so that in the intermediate coverage range the shift of the peaks is even enlarged by the values given in Fig. 2. This enlargement is depicted in Fig. 4, in which the shift of the Cd $4d_{5/2}$ maximum is given with respect to the position for the pristine Cd(Zn)Te as derived from the raw data (lower curve) and after the correction for the SPV (upper curve). Above 0.8 Å, the formation of the quaternary compound Cd(Zn,Mn)Te is accompanied by the formation of a metallic overlayer, inducing a downward band bending of $\approx 0.50 \pm 0.05$ eV (after SPV correction). At a nominal Mn coverage of 2 Å the band bending is completely developed and remains constant for further deposition steps up to 30 Å. Very similar results have been obtained from the Cd $3d$ core levels (not shown) and can be derived for the Mn $3d$ contribution at $E_B \approx 4$ eV (see Fig. 1). For Mn coverages above 30 Å no Cd photoemission from the substrate could be detected due to the limited photoemission information depth. Hence no further information on the band bending behavior can be deduced for thick Mn overlayers.

Note that the downward band bending derived from the Cd $3d$ and $4d$ levels is consistent with the observed SPV effect, since a downward band bending will force the electrons to accumulate at the surface, while the holes will dissolve into the bulk. Hence, the surface will be negatively charged and the photoemission spectrum will be shifted towards higher kinetic energies, leading to the detection of

electrons above the Fermi energy of the instrument.

The photoemission spectra of the Te $4d_{3/2}$ and $4d_{5/2}$ core levels are shown in Fig. 5. Again, the spectral features are shifted towards higher binding energies with increasing Mn coverage due to the downward band bending. As is the case of the Cd levels, the shift towards higher binding energies is further increased after correction for the SPV effect. A second Te species at lower binding energies evolves in the intermediate coverage range ($\geqslant$0.8 Å), which is at variance with a recent study of the Mn/$Cd_{0.96}Zn_{0.04}$Te(111) interface.[55] This discrepancy may be due to the different surface orientation/preparation and/or the improved experimental resolution in the present study. For large coverages ($\geqslant$ 30 Å), significant Te intensity can still be detected, even though the nominal Mn coverage is by far larger than the information depth [note that at $h\nu = 90$ eV the kinetic energy of the Te 4*d* levels is close to the minimum of electron escape depth at 40 eV (Ref. 5)]. After a short (5 min) sputter step removing just a few atomic layers the Te signal is completely suppressed and an elemental metallic Mn overlayer is detected. Obviously, a significant amount of Te segregates to the surface of the metallic Mn film. A comparison with the Te 4*d* peak area of the pristine surface reveals a Te overlayer thickness of approximately 4 Å for the spectrum with a nominal Mn coverage of 120 Å.

This finding sheds new light also on the initial stages of the interface formation: for small Mn coverages the interdiffusion should be regarded as a Te segregation effect rather than an in-diffusion of Mn and a replacement of Cd atoms by Mn atoms;[33,40] a segregation effect in compound semiconductor-metal interfaces is not unusual.[56] Moreover, Te has been used as a surfactant in III-V semiconductor epitaxial layers.[57] Several investigations of noble-metal interfaces with CdTe, (Cd,Hg)Te, or HgTe report on Te segregation.[34–38] This is consistent with our findings that a significant amount of Te remains on the surface throughout the whole interface formation process.

An unambiguous interpretation of the second Te species in the intermediate coverage range, however, is difficult. An influence of Zn can probably be neglected, since the nominal content is small and the Zn signal is rapidly attenuated by increasing Mn coverage (see below). No second phase can be detected for the Cd 4*d* levels or in the Cd *MNN* Auger spectra (see below, Fig. 8), thus suggesting that the second phase solely consists of Mn and Te. Niles *et al.* have investigated the epitaxial growth of MnTe on CdTe(110).[32] They report on a chemical shift of the Te 4*d* levels from CdTe to MnTe towards higher binding energies, in contrast to the second phase detected in our study. However, we expect the second phase to form on top of a metallic Mn layer, so that a core level shift in the MnTe layer could be influenced by the (underlying) metallic Mn layer. Furthermore, the metal-induced downward band bending only affects Te atoms within the Cd(Zn,Mn)Te interface and the Cd(Zn)Te bulk, hence leading to a shift towards higher binding energy only for these Te atoms. The same arguments could be applied for elemental Te as well, for which, according to the data collection of Wagner, a shift should be detected towards *higher* binding energies going from CdTe to Te.[59] While the formation of a MnTe overlayer still seems the most probable explanation, an unambiguous proof has yet to be found. Throughout this paper, we will hence denote the second species as the ''Mn-Te species.''

In the above discussion we have stated that segregated Te is present throughout the interface formation. This behavior is depicted in Fig. 6 in which the peak areas of the Cd and Te 4*d* features are plotted against the nominal Mn thickness. The peak areas were normalized by the peak areas from the pristine Cd(Zn)Te surface. While the attenuation of the Te signal is small for coverages up to 10 Å and above, two different intensity behaviors can be observed for the Cd signal. Up to 1 Å, the Cd signal is rapidly reduced, while for coverages above 1 Å a much smaller decrease is detected. The Cd attenuation is, however, always larger than that of

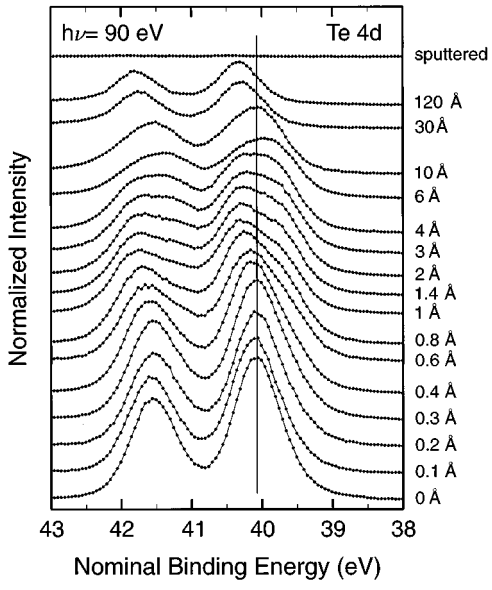

FIG. 5. Photoemission spectra of the Te 4*d* levels ($h\nu = 90$ eV). In the intermediate Mn-coverage range (0.8 Å–10 Å), a second Te phase begins to be formed at lower binding energies. All spectral features are shifted towards higher binding energy with increasing Mn deposition due to band bending. Even at high Mn coverages, significant Te emission is detected, which is completely eliminated after short sputter treatment.

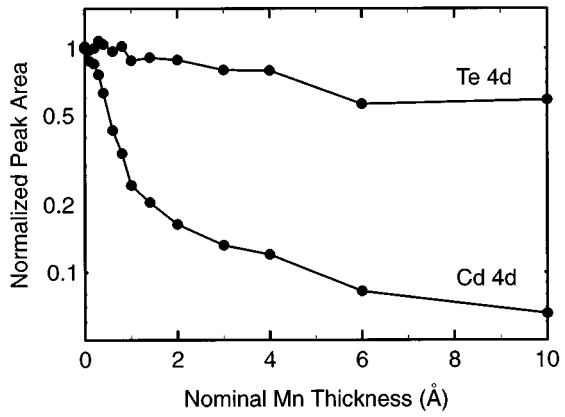

FIG. 6. Intensity attenuation of the Cd and Te 4*d* photoemission features of Figs. 3 and 5 for increasing Mn coverages ($\pm$10 %). The normalized peak areas are referred to as the pristine Cd(Zn)Te surface.

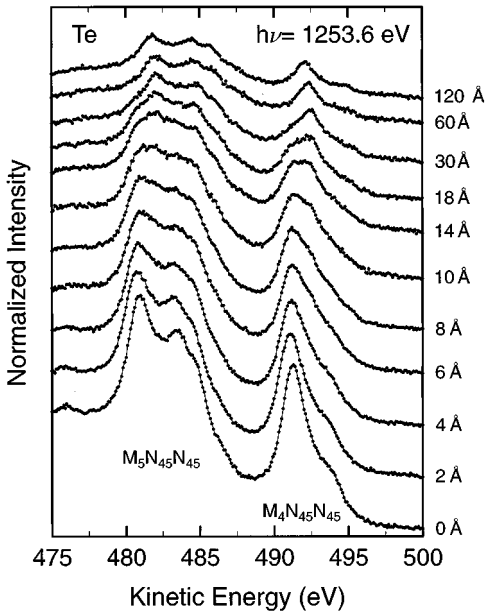

FIG. 7. Te $M_5N_{45}N_{45}$ and $M_4N_{45}N_{45}$ Auger spectra for increasing Mn coverage obtained with Mg $K\alpha$ irradiation. In the intermediate-coverage range, a second Te species begins to be formed.

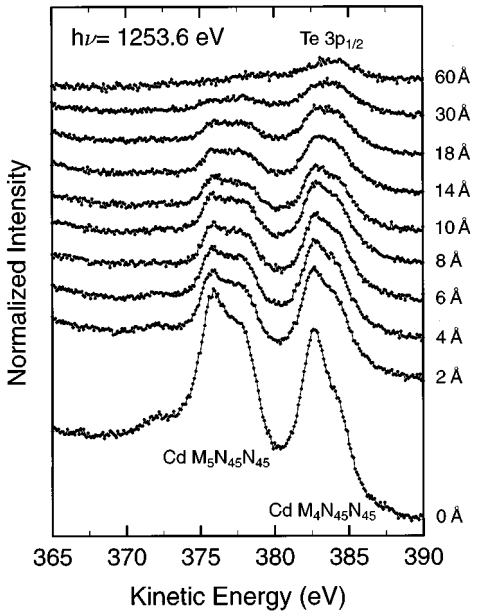

FIG. 8. Cd $M_5N_{45}N_{45}$ and $M_4N_{45}N_{45}$ Auger spectra as well as Te $3p_{1/2}$ photoemission for increasing Mn coverage obtained with Mg $K\alpha$ irradiation. Throughout the interface formation, no evidence for a second Cd species is found.

Te, with the consequence that only Te atoms are detected within the photoemission information volume for large Mn coverages (120 Å). Very similar results are obtained for the $3d_{3/2}$ levels of Cd and Te, thus ruling out explanations based on the Zn $3d$ and Te $5s$ contributions to the Cd $4d$ peak area or on different information depths for Cd and Te. Furthermore, both, the Te $3d_{3/2}$ and $4d$ levels are detected at lower kinetic energies than the respective Cd levels, so that a smaller information depth would be expected for the Te signal. The Zn signal shows a qualitatively similar attenuation behavior as the Cd signal as derived for the Zn $2p_{3/2}$ level from an investigation with Mg $K\alpha$ excitation. Thus, as stated above, a Te segregation rather than Mn indiffusion can clearly be derived from our experiments.

In order to gain more insight into the formation of the Mn-Te species in the intermediate-coverage range, we have also recorded Te $M_5N_{45}N_{45}$ and $M_4N_{45}N_{45}$ Auger spectra using Mg $K\alpha$ irradiation (Fig. 7). In the Auger case, the final state contributions to the detected peak position can be about 3 times larger due to the double-hole final state as compared to the photoemission case (one-hole final state). [58] Thus it is not surprising to detect the formation of the second Te species (i.e., the Mn-Te species) in the intermediate coverage range of the Auger spectra as a shift approximately twice as large as in the photoemission case (the formation of the second phase is most easily seen in the $M_4N_{45}N_{45}$ spectra at a kinetic energy of 490–495 eV). Again, significant Te emission can be detected for large nominal Mn coverages. The spectra for high nominal Mn coverages are shifted towards smaller kinetic energies due to the SPV effect. Between the 30 Å and the 120 Å spectra, the shift is ≈ 0.4 eV, which is comparable to the values derived from the above Fermi edge investigation with synchrotron radiation. This is not surprising, since the magnitude of the SPV effect depends only logarithmically on the incident photon flux.[51]

Since no Te Auger peak position data are reported for MnTe (Ref. 59) and changes in both, initial state binding energy and final state effects can be induced by the underlying metallic Mn layer, a rigorous identification of the secondary phase is hardly possible. However, the two times larger shift in the Auger spectra clearly indicates a considerable screening contribution, probably by the metallic underlayer, hence supporting the above interpretation of the Mn-Te species as MnTe. In addition, the Cd $M_5N_{45}N_{45}$ and $M_4N_{45}N_{45}$ Auger spectra in Fig. 8 support the assumption that Cd is not involved in the formation of this secondary (Mn-Te) phase: no significant shifts or changes in line shape of the $M_5N_{45}N_{45}$ peak are detected, even though large differences in line position were reported among elemental Cd and different Cd-group VI compounds.[59] Note that the $CdM_4N_{45}N_{45}$ Auger peak is superposed on the Te $3p_{1/2}$ photoemission peak, so that an enhanced intensity is detected at $E_{\mathrm{kin}} \approx 384$ eV even in the high-coverage spectrum (60 Å). This is again due to the fact that a significant amount of Te atoms floats atop the Mn overlayer, while the emission from Cd atoms is completely suppressed. The superposition of the $M_4N_{45}N_{45}$ and Te $3p_{1/2}$ peaks is also obvious from the increased area of the $M_4N_{45}N_{45}$ peak, as compared to reference spectra for elemental Cd (Ref. 60) and to the Te Auger spectra in Fig. 7, and from the enhanced shoulder of the $M_4N_{45}N_{45}$ peak at higher kinetic energy.

The Mn $3s$ core level spectra for increasing Mn coverage are presented in Fig. 9. Three different effects are observed. First we find a significant shift of the Mn $3s$ main line towards smaller binding energy for the first five Mn deposition steps. This shift is attributed to the formation of a second Mn species, as will be discussed below (Fig. 10). While the peak position of the 2 Å spectrum is mainly representative for Mn in the Cd(Zn,Mn)Te compound, the second species is associated with the metallic Mn overlayer. Note that the metal-

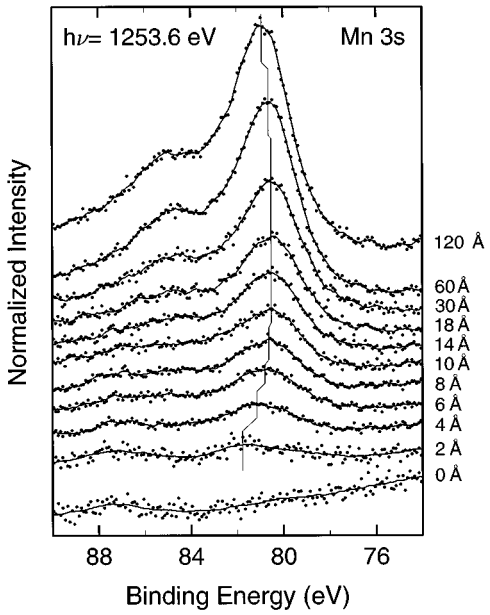

FIG. 9. Mg $K\alpha$ photoemission spectra of the Mn 3*s* core level with increasing Mn coverage. For a discussion of the satellite structure at $E_B \approx$ 85 eV and the shifts of the main peak see text.

induced band bending of the Cd and Te core levels is not effective for the Mn core levels of the overlayer atoms. Second, the Mn 3*s* main peak is shifted towards higher binding energy for high Mn coverages. This is due to the reduction of the SPV effect for thick metallic overlayers, as observed for the Cd and Te core levels as well. Finally, a satellite structure at $E_B \approx 85$ eV can be detected in the high-coverage regime. This structure is of interest because a derivation of magnetic properties of the Mn atoms (e.g., the local magnetic moment) based on the energy separation and intensity

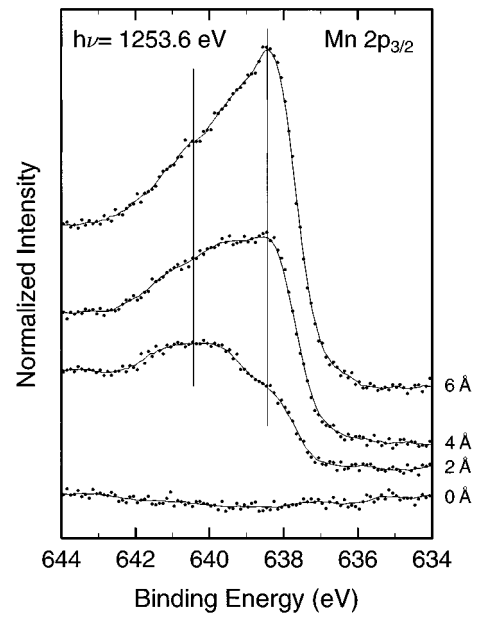

FIG. 10. Mg $K\alpha$ photoemission spectra of the Mn $2p_{3/2}$ core level for nominal Mn coverages up to 6 Å, revealing at least two different Mn species.

of this satellite structure has been attempted.[61–63] In our case, such an approach seems hardly possible, since the determination of the satellite intensity is obscured by the background feature at $E_B \approx 87.5$ eV, which is presumably due to Zn $3p_{3/2}$ emission. Within this limitation, however, no significant changes of the satellite intensity or energy are observed with increasing Mn coverage. Furthermore, the validity of such an approach is questionable, which also has been pointed out by van Acker *et al.*[64] They showed in a careful study of the Fe 3*s* core level in different compounds and alloys that there is a poor correlation between magnetic moment and Fe 3*s* splitting or satellite intensity ratios, and that even Pauli paramagnets exhibit 3*s* splitting. They argue that too many effects contribute to the intensity ratio and energy separation for a simple correlation with the local magnetic moments.

As mentioned above, further evidence for the formation of a Cd(Zn,Mn)Te quaternary compound can be derived from the existence of two Mn species in the low-coverage regime. In addition to the Mn 3*s* shift of Fig. 9, these two species can be detected in the Mn $2p_{3/2}$ core level spectra of Fig. 10. Here, only spectra for the first three deposition steps are presented. Clearly, a Mn species associated with the quaternary Cd(Zn,Mn)Te compound at $E_B \approx 640.5$ eV can be distinguished from the metallic Mn species at $E_B \approx 638.4$ eV. It is not quite clear from the present data whether the broad structure around 640.5 eV actually represents one or more distinct Mn species associated with the quaternary interface compound or whether various satellites contribute to the spectrum such that the observed ''multipeak'' structure results. A decision is presently impossible since the satellites of the $2p_{3/2}$ peaks are expected to be very different from those of the 3*s* peaks.[61] The line position for the metallic species remains constant until the reduction of SPV effect becomes effective for high Mn coverages, leading to a final peak position of $E_B \approx 638.8$ eV (not shown). Note that at a nominal coverage of 2 Å approximately equal intensity is observed for both species (after background subtraction). This is in good agreement with the existence of a Fermi edge for Mn coverages $\geqslant 1$ Å and with the fact that the formation of the quaternary Cd(Zn,Mn)Te compound is apparently completed at that stage of the Mn/Cd(Zn)Te interface formation.

IV. CONCLUDING DISCUSSION

The experimental findings of the preceding section are summarized in a layer model depicted in Fig. 11 (all layer thicknesses given pertain to the deposition series of Figs. 1, 3, and 5). For low nominal Mn coverages (below 1 Å), the absence of a Fermi edge in the valence-band spectra suggests an interdiffused, quaternary Cd(Zn,Mn)Te semiconductor in the surface region. This is corroborated by the attenuation behavior of the Cd, Zn, and Te signals: interdiffusion processes take place in the low-coverage regime, in which the Cd and Zn signals of the previously Cd-terminated surface are rapidly attenuated and the Te-segregation starts.

In the intermediate-coverage range (1–10 Å Mn) a metallic Mn layer is formed, inducing a band bending in the underlying quaternary compound. This is derived from the evolution of a metallic Fermi edge, from the Cd core and

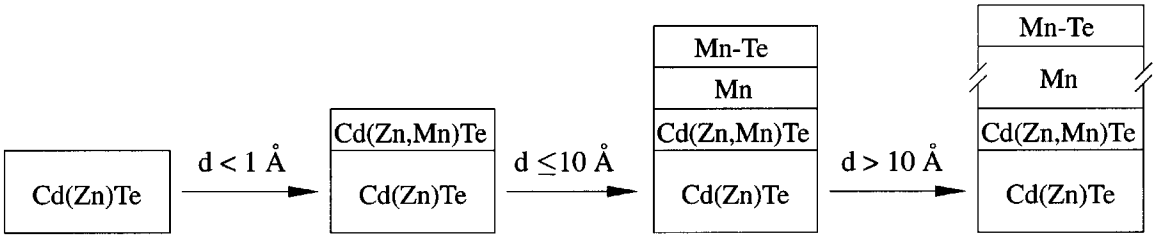

FIG. 11. Schematic layer model of the Mn/Cd(Zn)Te interface formation as a function of nominal Mn thickness d. Below 1 Å, an interdiffused quaternary semiconductor is formed near the surface. Up to 10 Å, a metallic Mn layer with an additional, Mn- and Te-containing species is detected. For thicker Mn layers, the segregation of Te is observed, which can be completely removed by short sputter treatment. The nominal Mn thicknesses given pertain to the synchrotron measurements of Figs. 1, 3, and 5.

shallow valence level shifts, and from the existence of a surface photovoltage effect. Simultaneously, a Mn-Te species is formed, as seen in the photoemission spectra of the Te $4d$ core level. As discussed above, this species is difficult to assign, but the formation of manganese telluride (MnTe) seems most likely. The Mn-Te species is identified as located on top of the metallic Mn layer for several reasons. First, we find a significant Te segregation to the surface even for large Mn coverages. Second, the observed band bending is derived from the Cd photoemission signal, i.e., the band bending and the SPV effect are induced at an interface where Cd atoms are present. This can, however, only be the case if the metallic Mn layer grows on top of the quaternary Cd(Zn,Mn)Te compound, thus ruling out the presence of a Mn-Te species at this interface. Third, the Mn-Te species becomes dominant in the upper Mn-coverage regime, while on the contrary the Mn $3d$-derived valence region emission feature at $\approx$ 4 eV is attenuated by the increasing Mn overlayer. This valence feature is thus assigned to the Cd(Zn,Mn)Te quaternary compound. Finally, short sputtering immediately removes the second Te species found on thick Mn films. These observations unambiguously lead to the conclusion that the Mn-Te species is located on top of the Mn layer.

The presence of Te on top of the Mn film and the complete removal of Te atoms from the Mn film surface by a short sputter-treatment gives strong evidence for a significant Te segregation during interface formation. After the sputter step, only Mn atoms within a metallic surrounding can be detected. Obviously, a purely metallic Mn film exists inbetween the Cd(Zn,Mn)Te quaternary semiconductor compound and the Mn-Te overlayer.

According to this layer model, three nominal Mn coverages are of particular interest for the determination of the (schematic) electronic structure of the interface (Fig. 12): at 0 Å nominal Mn coverage, the pristine Cd(Zn)Te surface is characterized by the energetic difference of 0.80 eV ($\pm$0.10 eV) between valence-band maximum (VBM) and Fermi energy (i.e., the reference level in our photoemission experiment), as derived from a linear extrapolation of the valence-band edge. The binding energy of the Cd $4d_{5/2}$ level (with respect to E_F) is regarded as representative of changes in the band bending of the substrate and is derived as 10.80 eV ($\pm$0.05 eV) in this case.

For a nominal coverage of 0.8 Å Mn, no Fermi edge is yet detected. At this point, the quaternary Cd(Zn,Mn)Te surface is investigated. The formation of the quaternary compound leads to an upward shift of the VBM by 0.10 eV (i.e., E_F-VBM = 0.70 eV) and a downward shift of the core levels by 0.15 eV [E_B(Cd $4d_{5/2}$) = 10.95 eV]. This finding suggests a shift of the Fermi energy within the semiconductor and/or a decrease of the band gap. The latter interpretation would be in contradiction to the increase of the band gap in the order CdTe-ZnTe-MnTe, i.e., with band gap widening due to the alloying of Cd(Zn)Te with Mn.[1,65,66,69] The downward shift of the Cd $4d_{5/2}$ level can be interpreted either as a chemical shift due to the change of the environment induced by the Mn alloying or by a change of the surface band bending due to an altered surface density of states.

At nominally 6 Å Mn, the metallic Mn layer on top of the Cd(Zn,Mn)Te compound is formed and the band bending induced by the metal-semiconductor interface is fully established. Taking the SPV effect into account, one arrives at a further downward shift of the Cd $4d_{5/2}$ core level by 0.35 eV [E_B(Cd $4d_{5/2}$) = 11.30 eV]. Of course, no VBM of the Cd(Zn,Mn)Te can be derived from the spectrum at a Mn coverage of 6 Å. However, no changes in the band gap are expected once interdiffusion becomes negligible and the formation of a metallic Mn layer begins. Thus, the (virtual) VBM for a nominal Mn coverage of 6 Å can be well approximated by the VBM position of the 0.8 Å Mn measurement, corrected by the band bending as derived from the Cd $4d_{5/2}$ level. We then arrive at a (virtual) energy difference between the VBM and the Fermi energy of 1.05 ($\pm$0.10) eV. This value represents the potential barrier to be overcome by holes on their way from the metallic Mn layer into the

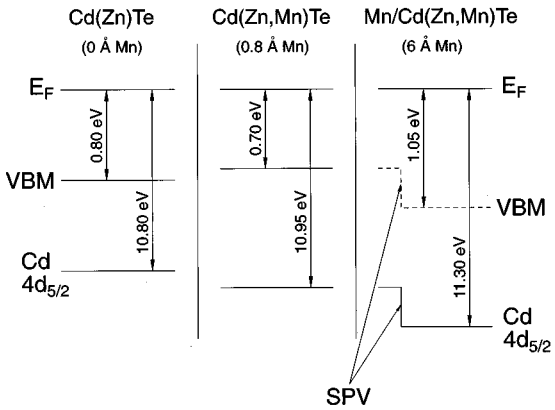

FIG. 12. Schematic model of the electronic structure at different stages of the Mn/Cd(Zn)Te interface formation: pure Cd(Zn)Te (0 Å Mn), interdiffused Cd(Zn,Mn)Te (0.8 Å Mn), and the Mn/Cd(Zn,Mn)Te Schottky barrier (6 Å Mn). An E_F-VBM difference of 1.05 eV is derived for the last case after the surface photovoltage correction.

Cd(Zn,Mn)Te quaternary semiconductor. In order to derive a Schottky barrier for the electrons (i.e., the difference between the conduction-band minimum and the Fermi energy) from our data, one is forced to assume a value for the band gap of the interdiffused Cd(Zn,Mn)Te compound. This is, however, a difficult task since the exact concentration of Mn and Zn within the sample volume determining the (surface) band gap is unknown and most likely inhomogeneous as well. Both, the alloying with Zn [thus forming Cd(Zn)Te][65] and with Mn [forming Cd(Mn)Te][66] increases the band gap of pure CdTe (around 1.5 eV at room temperature[67,68]), as is also true for the quaternary compound.[69] Thus, a band gap in the range of 1.5 to 2.0 eV seems feasible and leads to a Schottky barrier range of 0.45–0.95 eV. Overall, a downward change in band bending of 0.5 eV is detected between the pristine Cd(Zn)Te surface and the fully established Mn/Cd(Zn,Mn)Te interface.

These results can be well compared to Schottky barriers and E_F-VBM values for other metals on CdTe: John *et al.* report E_F-VBM = 0.96 eV for the Ag/CdTe(100) interface.[39] Friedman *et al.* derived E_F-VBM values in the range of 0.8–1.0 eV for Ag, Cu, and Au interfaces with both *n*- and *p*-type CdTe(110), thus detecting a Fermi-level pinning consistent with a defect or Tersoff-type model of Schottky barrier formation.[38] Patterson *et al.* obtained Schottky barriers from 0 to 1.0 eV for a wide range of metals (In, Ag, Al, Sn, Cu, Au, Ni) on CdTe(110),[70] while the α-Sn/CdTe(100) interface is reported with a Schottky barrier height of 0.55 eV.[71] Moreover, Vos *et al.* report Schottky barriers from 0.5 to 1.5 eV for various (non-Mn) metals on ZnSe(100) surfaces.[72] Shaw *et al.* have pointed out that in the case of Au or In on CdTe(110) the pinned Fermi-level position is determined by bulklike defects.[73]

Unfortunately, no barrier data are given by Wall *et al.* for the interdiffused Mn/CdTe(110) interface[33]. In clear contrast to our results, but on a different surface, Dharmadasa *et al.* have reported an Ohmic contact for Mn/CdTe(110), i.e., the absence of a Schottky barrier for vacuum-cleaved, air-cleaved, and chemically etched CdTe surfaces.[74] Our results clearly show the existence of a Schottky barrier, even though the absolute value is inaccurate due to the uncertainty in band gap determination. However, even for the smallest possible band gap (approximately 1.5 eV for pure CdTe), a Schottky barrier height of about 0.5 eV would be derived. Thus, an Ohmic contact can clearly be ruled out for the case of Mn on Cd(Zn,Mn)Te(100).

V. SUMMARY

Several interesting effects beyond a simple and abrupt metal-semiconductor interface formation have been found for the Mn/Cd(Zn)Te(100) interface using synchrotron- and Mg $K\alpha$-excited photoemission and Auger electron spectroscopy. For small nominal Mn coverages (below 1 Å Mn), an interdiffused, quaternary Cd(Zn,Mn)Te compound semiconductor interface is formed. Minimization of the surface free energy leads to a segregation of Te to the previously Cd-terminated polar surface. In the intermediate-coverage range, a metallic Mn film is formed on top of the Cd(Zn,Mn)Te compound, inducing a downward band bending in the substrate and giving rise to a surface photovoltage effect. In this coverage regime, a second, Te and Mn containing species is formed on top of the Mn layer. Throughout the interface formation, significant Te segregation is detected up to a nominal Mn thickness as high as 120 Å, while no Te atoms are present within the metallic Mn film. The valence-band maximum of Cd(Zn,Mn)Te at the interface with a metallic Mn film has been determined as 1.05 ($\pm$ 0.10) eV below the Fermi energy as compared to 0.7 eV for the Cd(Zn,Mn)Te surface and 0.8 eV for the pristine Cd(Zn)Te surface.

ACKNOWLEDGMENTS

We would like to thank the BESSY staff for technical support. Financial support by the Deutsche Forschungsgemeinschaft through SFB410 is gratefully acknowledged. One of us (E.U.) is grateful to the Fond der Chemischen Industrie for financial support.

[1] *Semiconductors. Physics of II-VI and I-VII Compounds, Semimagnetic Semiconductors*, edited by K.-H. Hellwege and O. Madelung, Landolt-Börnstein, New Series, Group III, Vol. 17, Pt. b (Springer, Berlin 1982).

[2] See, e.g., A. Wall, C. Caprile, A. Franciosi, M. Vaziri, R. Reifenberger, and J. K. Furdyna, J. Vac. Sci. Technol. A **4**, 2010 (1986), and references therein.

[3] C. Heske, U. Winkler, R. Fink, E. Umbach, Ch. Jung, P. R. Bressler, and Ch. Hellwig, *The Physics of Semiconductors*, edited by M. Scheffler and R. Zimmermann (World Scientific, Singapore, 1996), p. 823.

[4] H. Neureiter, S. Spranger, M. Sokolowski, and E. Umbach, Surf. Sci. (to be published).

[5] C. Heske, U. Winkler, R. Fink, E. Umbach, Ch. Jung, P. R. Bressler, and Ch. Hellwig, this issue, Phys. Rev. B **56**, 2070 (1997).

[6] C. Heske, U. Winkler, H. Neureiter, M. Sokolowski, R. Fink, E. Umbach, Ch. Jung, and P. R. Bressler, Appl. Phys. Lett. **70**, 1022 (1997).

[7] G. K. Averkieva, M. E. Bolko, N. N. Konstantinova, T. B. Popova, V. D. Prochukhan, and Yu. V. Rud' Fiz. Tverd Tela (Leningrad) **34**, 1222 (1992) [Sov. Phys. Solid State **34**, 1222 (1992)].

[8] A. Franciosi, Shu Chang, R. Reifenberger, U. Debska, and R. Riedel, Phys. Rev. B **32**, 6682 (1985).

[9] A. Franciosi, C. Caprile, and R. Reifenberger, Phys. Rev. B **31**, 8061 (1985).

[10] J. K. Furdyna, J. Vac. Sci. Technol. A **4**, 2002 (1986).

[11] J. K. Furdyna, J. Appl. Phys. **64**, R29 (1988).

[12] B. E. Larson, K. C. Hass, H. Ehrenreich, and A. E. Carlsson, Solid State Commun. **56**, 347 (1985).

[13] B. A. Orlowski, K. Kopalko, and W. Chab, Solid State Commun. **50**, 749 (1984).

[14] M. Taniguchi, M. Fujimori, M. Fujisawa, T. Mori, I. Souma, and Y. Oka, Solid State Commun. **62**, 431 (1987).

[15] M. Taniguchi, K. Soda, I. Souma, and Y. Oka, Phys. Rev. B **46**, 15 789 (1992).

[16] A. Wall, C. Caprile, and A. Franciosi, R. Reifenberger, and U. Debska, J. Vac. Sci. Technol. A **4**, 818 (1986).
[17] A. Wall, S. Chang, P. Philip, C. Caprile, and A. Franciosi, R. Reifenberger, and F. Pool, J. Vac. Sci. Technol. A **5**, 2051 (1987).
[18] R. Weidemann, H. -E. Gumlich, M. Kupsch, H. -U. Middelmann, and U. Becker, Phys. Rev. B **45**, 1172 (1992).
[19] V. Cháb, G. Paolucci, K. C. Prince, M. Surman, and A. M. Bradshaw, Phys. Rev. B **38**, 12 353 (1988).
[20] S.-K. Chang, A. V. Nurmikko, J.-W. Wu, L. A. Kolodziejski, and R. L. Gunshor, Phys. Rev. B **37**, 1191 (1988).
[21] R. D. Feldman, R. L. Opila, and P. M. Bridenbaugh, J. Vac. Sci. Technol. A **3**, 1988 (1985).
[22] A. Franciosi, A. Wall, Y. Gao, J. H. Weaver, M. -H. Tsai, J. D. Dow, R. V. Kasowski, R. Reifenberger, and F. Pool, Phys. Rev. B **40**, 12 009 (1989).
[23] L. Ley, M. Taniguchi, J. Ghijsen, R. L. Johnson, and A. Fujimori, Phys. Rev. B **35**, 2839 (1987).
[24] P. Oelhafen, M. P. Vecchi, J. L. Freeouf, and V. L. Moruzzi, Solid State Commun. **44**, 1547 (1982).
[25] M. Taniguchi, L. Ley, R. L. Johnson, J. Ghijsen, and M. Cardona, Phys. Rev. B **33**, 1206 (1986).
[26] M.-H. Tsai, John D. Dow, R. V. Kasowski, A. Wall, and A. Franciosi, Solid State Commun. **69**, 1131 (1989).
[27] A. Waag, S. Schmeusser, R. N. Bicknell-Tassius, D. R. Yakovlev, W. Ossau, and G. Landwehr, Appl. Phys. Lett. **59**, 2995 (1991).
[28] A. Wall, A. Franciosi, Y. Gao, J. H. Weaver, M.-H. Tsai, J. D. Dow, and R. V. Kasowski, J. Vac. Sci. Technol. A **7**, 656 (1989).
[29] S.-H. Wei and A. Zunger, Phys. Rev. B **35**, 2340 (1987).
[30] G. M. Williams, A. G. Cullis, C. R. Whitehouse, D. E. Ashenford, and B. Lunn, Appl. Phys. Lett. **55**, 1303 (1989).
[31] P. R. Bressler and H.-E. Gumlich, J. Cryst. Growth **138**, 1028 (1994).
[32] D. W. Niles, H. Höchst, and M. S. Engelhardt, J. Electron Spectrosc. Relat. Phenom. **52**, 139 (1990).
[33] A. Wall, A. Raisanen, G. Haugstad, L. Vanzetti, and A. Franciosi, Phys. Rev. B **44**, 8185 (1991).
[34] G. D. Davis, W. A. Beck, N. E. Byer, R. R. Daniels, and G. Margaritondo, J. Vac. Sci. Technol. A **2**, 546 (1984).
[35] G. D. Davis, N. E. Byer, R. A. Riedel, and G. Margaritondo, J. Appl. Phys. **57**, 1915 (1985).
[36] A. Franciosi, P. Philip, and D. J. Peterman, Phys. Rev. B **32**, 8100 (1985).
[37] D. J. Friedman, G. P. Carey, I. Lindau, and W. E. Spicer, Phys. Rev. B **34**, 5329 (1986).
[38] D. J. Friedman, I. Lindau, and W. E. Spicer, Phys. Rev. B **37**, 731 (1988).
[39] P. John, T. Miller, T. C. Hsieh, A. P. Shapiro, A. L. Wachs, and T. -C. Chiang, Phys. Rev. B **34**, 6704 (1986).
[40] N. Happo, H. Sato, K. Mimura, S. Hosokawa, M. Taniguchi, Y. Ueda, and M. Koyama, Phys. Rev. B **50**, 12 211 (1994).
[41] H. Petersen, C. Jung, C. Hellwig, W. B. Peatman, and W. Gudat, Rev. Sci. Instrum. **66**, 1 (1995).
[42] S. Tatarenko, F. Bassani, J. C. Klein, K. Saminadayar, J. Cibert, and V. H. Etgens, J. Vac. Sci. Technol. A **12**, 140 (1994).
[43] M. B. Veron, M. Sauvage-Simkin, V. H. Etgens, S. Tatarenko, H. A. Van Der Vegt, and S. Ferrer, Appl. Phys. Lett. **67**, 3957 (1995).
[44] D. W. Niles and H. Höchst, Phys. Rev. B **43**, 1492 (1991).
[45] D. W. Niles and H. Höchst, Phys. Rev. B **46**, 1498 (1992).
[46] H. Sato, N. Happo, J. Harada, M. Taniguchi, and Y. Ueda, Cryst. Res. Technol. **31**, 329 (1996).
[47] N. Happo, H. Sato, J. Harada, T. Mihara, M. Taniguchi, and Y. Ueda, J. Electron Spectrosc. Relat. Phenom. **80**, 213 (1996).
[48] X. Jin, M. Zhang, G. S. Dong, Y. Chen, M. Xu, X. G. Zhu, X. Wang, E. D. Lu, H. B. Pan, P. S. Xu, X. Y. Zhang, and C. Y. Fan, Phys. Rev. B **50**, 9585 (1994).
[49] X. Jin, Y. Chen, G. S. Dong, M. Zhang, M. Xu, X. G. Zhu, X. Wang, E. D. Lu, H. B. Pan, P. S. Xu, X. Y. Zhang, and C. Y. Fan, Phys. Rev. B **51**, 9702 (1995).
[50] M. Alonso, R. Cimino, and K. Horn, Phys. Rev. Lett. **64**, 1947 (1990).
[51] M. H. Hecht, Phys. Rev. B **41**, 7918 (1990).
[52] K. C. Prince, G. Paolucci, V. Cháb, M. Surman, and A. M. Bradshaw, Surf. Sci. **206**, L871 (1988).
[53] H. Höchst, D. W. Niles, and I. Hernandez-Calderon, Phys. Rev. B **40**, 8370 (1989).
[54] C. Heske, U. Winkler, D. Eich, R. Fink, E. Umbach, Ch. Jung, and P. R. Bressler (unpublished).
[55] P. S. Xu, F. Y. Yang, S. H. Xu, E. D. Lu, X. J. Yu, and R. C. Fang, J. Electron Spectrosc. Relat. Phenom. **80**, 217 (1996).
[56] Zhangda Lin, F. Xu, and J. H. Weaver, Phys. Rev. B **36**, 5777 (1987).
[57] N. Grandjean, J. Massies, and V. H. Etgens, Phys. Rev. Lett. **69**, 796 (1992).
[58] J. C. Fuggle, E. Umbach, and D. Menzel, Solid State Commun. **20**, 89 (1976).
[59] C.D. Wagner, in *Practical Surface Analysis*, 2nd ed., edited by D. Briggs and M. P. Seah (Wiley, Chichester, 1990), Vol. 1, p. 595.
[60] C. D. Wagner, W. M. Riggs, L. E. Davis, J. F. Moulder, and G. E. Muilenberg, in *Handbook of X-Ray Photoelectron Spectroscopy*, edited by G. E. Muilenberg (Perkiu Elmer Corporation, Eden Prairie, Minnesota, 1979).
[61] A. S. Arrott, B. Heinrich, C. Liu, and S. T. Purcell, J. Magn. Magn. Mater. **54-57**, 1025 (1986).
[62] A. S. Arrott, B. Heinrich, S. T. Purcell, J. F. Cochran, and K. B. Urquhart, J. Appl. Phys. **61**, 3721 (1987).
[63] B. Heinrich, A. S. Arrott, C. Liu, and S. T. Purcell, J. Vac. Sci. Technol. A **5**, 1935 (1987).
[64] J. F. van Acker, Z. M. Stadnik, J. C. Fuggle, H. J. W. M. Hoekstra, K. H. J. Buschow, and G. Stroink, Phys. Rev. B **37**, 6827 (1988).
[65] K. Saito, A. Ebina, and T. Takahashi, Solid State Commun. **11**, 841 (1972).
[66] R. Bücker, H.-E. Gumlich, and M. Krause, J. Phys. C **18**, 661 (1985).
[67] G. L. Hansen, J. L. Schmit, and T. N. Casselman, J. Appl. Phys. **53**, 7099 (1982).
[68] C. Vázquez-López, H. Navarro, R. Aceves, and M. C. Vargas, J. Appl. Phys. **58**, 2066 (1985).
[69] R. Brun del Re, T. Donofrio, J. Avon, J. Majid, and J. C. Woolley, Nuovo Cimento **2D**, 1911 (1983).
[70] M. H. Patterson and R. H. Williams, J. Cryst. Growth **59**, 281 (1982).
[71] Ming Tang, D. W. Niles, I. Hernández-Calderón, and H. Höchst, Phys. Rev. B **36**, 3336 (1987).
[72] M. Vos, F. Xu, Steven G. Anderson, J. H. Weaver, and H. Cheng, Phys. Rev. B **39**, 10 744 (1989).
[73] J. L. Shaw, R. E. Viturro, L. J. Brillson, D. Kilday, M. K. Kelly, and G. Margaritondo, J. Vac. Sci. Technol. A **6**, 2752 (1988).
[74] I. M. Dharmadasa, W. G. Herrenden-Harker, and R. H. Williams, Appl. Phys. Lett. **48**, 1802 (1986).